Hypothesis-Conditioned Forecast of Hubble-Tension Relief

Assuming the GWTC-3 Dark-Siren Propagation Signal is Physical

Aiden B. Smith

February 10, 2026

Abstract

This work presents hypothesis-conditioned forecasts for the Hubble tension under the assumption that the O3 dark-siren modified-propagation anomaly is physical. The upstream anomaly analysis, archived on Zenodo (DOI: 10.5281/zenodo.18584705), reports $\Delta\mathrm{LPD}_{\mathrm{tot}} \simeq +3.67$, whereas a GR-truth injection calibration gives mean -0.839, standard deviation 0.240, and maximum $+0.076$ over 512 realizations. Posterior draws from the reconstructed modified-gravity model are propagated into late-time anchor observables, CMB-lensing forecasts, and compressed early-universe inversions.

In the constrained, repeatability-calibrated endpoint, the preferred anchor-based relief posterior is moderate: $\mathcal{R}^{\mathrm{GR}}_{\mathrm{anchor}}$ has mean 0.246 with p16/p50/p84 = 0.205/0.239/0.277, and the local-versus-high-z GR gap is typically $\sim 1.17\sigma$. A joint SN+BAO+CC transfer-bias fit with O3 metadata yields $\log \mathrm{BF}_{\mathrm{transfer/no-transfer}} = -0.533$, indicating no preference for explicit transfer terms in this setup.

For CMB signatures, CAMB-based propagation to Planck 2018 lensing bandpowers predicts suppressed lensing power, with median shifts of about -14.9% near $L \simeq 100$ and -8.4% near $L \simeq 300$ in a direct 16-draw pilot. Compressed $\theta_\star$ inversion under GR assumptions raises inferred H_0 relative to model truth: median inferred $H_0 \simeq 72.55$ (fixed Ω_m) or 75.34 (lensing-proxy Ω_m). Under the physical-signal hypothesis, partial tension relief is plausible, but decisive resolution requires full Boltzmann-level modified-gravity refits and independent siren data.

1 Motivation and Scope

The present analysis is conditional: it does not re-establish the O3 anomaly detection claim, but asks what follows if that signal is physical. The O3 anomaly replication repository is public on Zenodo (DOI: 10.5281/zenodo.18584705) and provides the calibrated baseline used here. The follow-up objective is to convert that hypothesis into quantitative predictions for:

1. late-time inferred-H_0 behavior,
2. transfer-bias robustness across SN+BAO+CC,
3. CMB-lensing and compressed early-universe inference shifts under GR interpretation.

2 Forecast Definitions

Posterior draws are taken from `outputs/finalization/highpower_multistart_v2/M0_start101` and propagated through synthetic anchor and CMB inference pipelines.

2.1 Late-time relief metrics

Define the baseline local-versus-Planck gap

$$\Delta H_0^{\rm base} \equiv \left| H_0^{\rm local} - H_0^{\rm Planck} \right|, \tag{1}$$

and the posterior-gap relief fraction

$$\mathcal{R}_{\rm post} \equiv 1 - \frac{\left| H_{0,\rm MG}^{\rm p50} - H_0^{\rm local} \right|}{\Delta H_0^{\rm base}}. \tag{2}$$

The preferred estimator is anchor-based. For each anchor redshift z_a, a synthetic $H(z_a)$ is generated under model truth and inverted with GR assumptions:

$$H_{0,\rm GR}(z_a) = \frac{H_{\rm obs}(z_a)}{\sqrt{\Omega_{m0}^{\rm GR}(1+z_a)^3 + (1-\Omega_{m0}^{\rm GR})}}. \tag{3}$$

The anchor-averaged relief statistic is

$$\mathcal{R}_{\rm anchor}^{\rm GR} \equiv 1 - \frac{\left| \overline{H_{0,\rm GR}} - H_0^{\rm local} \right|}{\Delta H_0^{\rm base}}. \tag{4}$$

2.2 CMB-focused tests

Two CMB-oriented tests are used:

1. draw-level propagation of $(H_0, \Omega_{m0}, \Omega_{k0}, \sigma_8)$ to Planck 2018 lensing bandpowers (template-proxy and direct CAMB modes),
2. compressed early-universe inversion using $\theta_\star = r_d/D_M(z_\star)$ under GR assumptions, with alternative assumptions for inferred Ω_m.

These tests target inference shifts and predicted signatures; they are not full TT/TE/EE Boltzmann likelihood refits.

3 Results

3.1 Late-time forecast and robustness

Using $z_a = \{0.2, 0.35, 0.5, 0.62\}$, 20,000 Monte Carlo replicates per anchor, and reference values $H_0^{\rm local} = 73.0 \pm 1.0$ and $H_0^{\rm Planck} = 67.4 \pm 0.5$:

- model-truth posterior gives $H_0^{\rm p50} \simeq 70.39$ (p16/p84 = 67.70/73.39),
- single-run posterior-gap relief is $\mathcal{R}_{\rm post} \simeq 0.534$,
- constrained endpoint gives $\mathcal{R}_{\rm anchor}^{\rm GR}$ mean 0.246 with p16/p50/p84 = 0.205/0.239/0.277,
- typical local-versus-high-z GR gap significance is $\sim 1.17\sigma$.

The joint transfer-bias fit over SN+BAO+CC (with O3 support as metadata) yields

$$\log {\rm BF}_{\rm transfer/no\text{-}transfer} = -0.533, \tag{5}$$

so explicit transfer terms are not preferred by these data in this configuration.

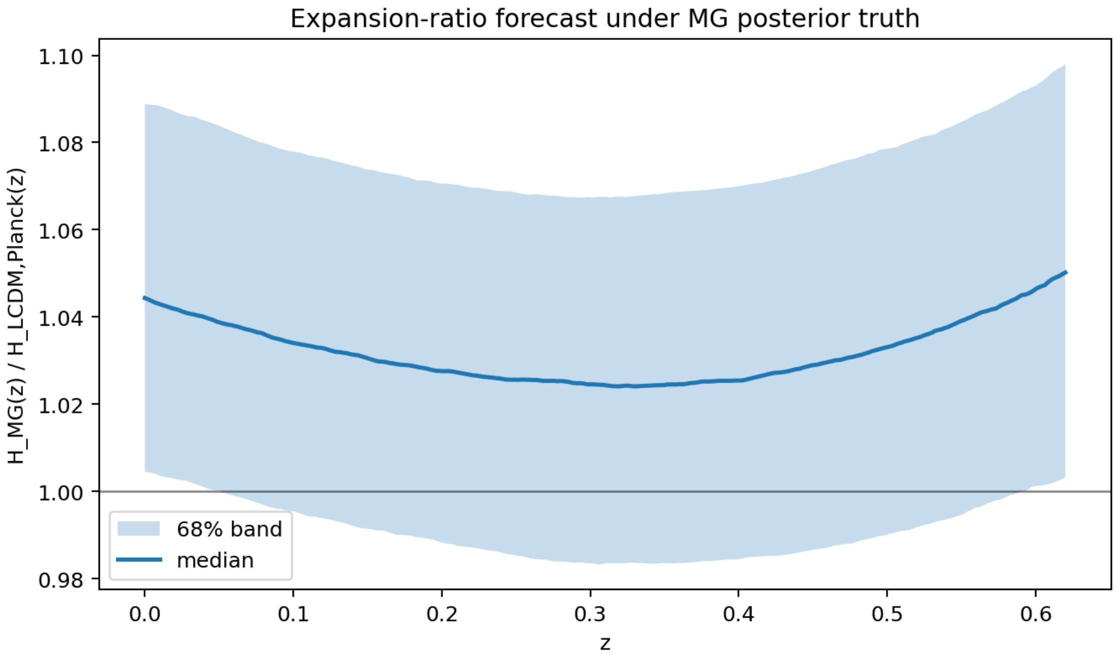

Figure 1: Forecasted expansion-ratio envelope under model truth: $H_{\rm MG}(z)/H_{\Lambda{\rm CDM,Planck}}(z)$.

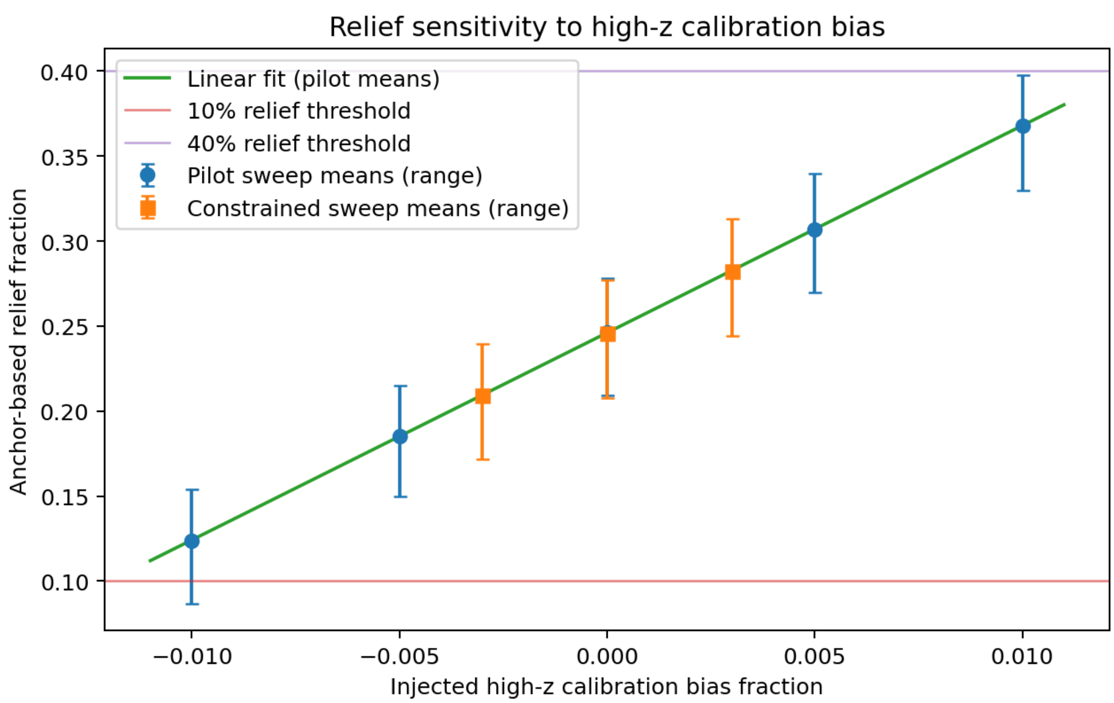

Figure 2: Anchor-based relief sensitivity to injected high-z calibration bias (pilot and constrained sweeps).

3.2 CMB lensing signature forecast

The direct CAMB pilot run (16 posterior draws, Planck 2018 lensing bandpowers) finds median suppression of the lensing spectrum relative to the Planck-reference model:

$$\left.\frac{C_L^{\phi\phi}(\mathrm{MG})}{C_L^{\phi\phi}(\mathrm{Planck\ ref})}\right|_{L\approx 100} \simeq 0.851, \qquad \left.\frac{C_L^{\phi\phi}(\mathrm{MG})}{C_L^{\phi\phi}(\mathrm{Planck\ ref})}\right|_{L\approx 300} \simeq 0.916. \tag{6}$$

In the same pilot, only 12.5% of draws outperform the Planck-reference model in lensing-bandpower χ^2.

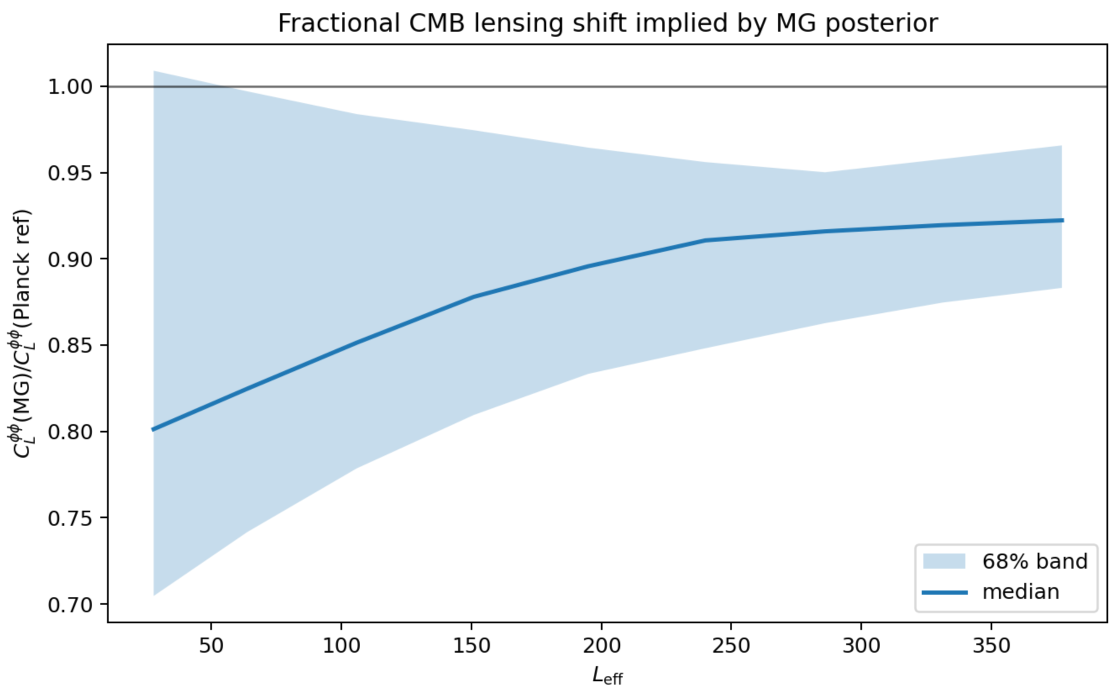

Figure 3: Predicted CMB lensing ratio $C_L^{\phi\phi}(\mathrm{MG})/C_L^{\phi\phi}(\mathrm{Planck\ ref})$ from the direct CAMB pilot.

3.3 Early-universe GR mis-inference test

Compressed $\theta_\star$ inversion under GR assumptions gives systematic upward shifts in inferred H_0 relative to model-truth draws:

- fixed-Planck Ω_m assumption: inferred H_0 mean 71.72, p50 72.55, mean $\Delta H_0 \equiv H_0^{\mathrm{inf}} - H_0^{\mathrm{true}} \simeq +1.14$ km s^{-1} Mpc^{-1},
- lensing-proxy Ω_m assumption: inferred H_0 mean 75.15, p50 75.34, mean $\Delta H_0 \simeq +4.57$ km s^{-1} Mpc^{-1}.

The implied sound-horizon shift required to force exact local-H_0 matching is modest in central tendency but broad in distribution: mean $\Delta r_d/r_d \approx -1.74\%$ (fixed-Ω_m mode) or $+2.92\%$ (lensing-proxy mode).

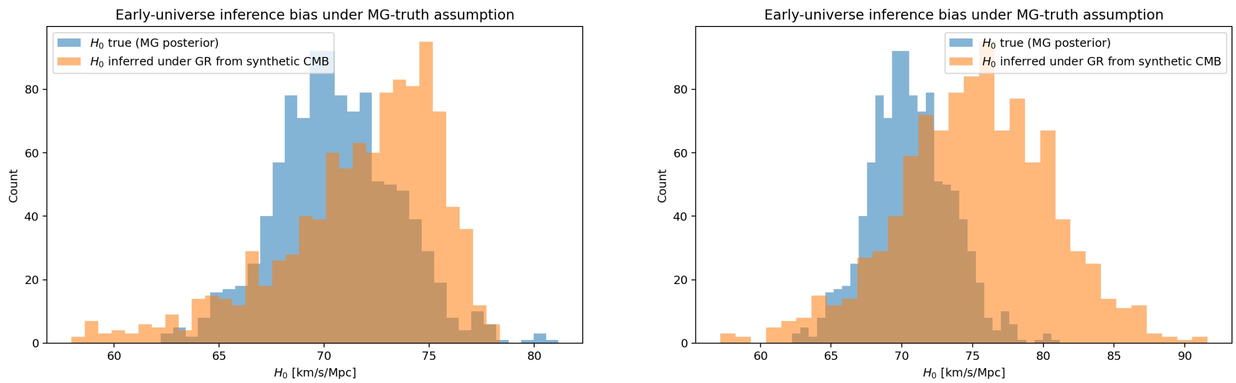

Figure 4: Histogram-level comparison of true and GR-inferred H_0 in compressed early-universe inversion tests. Left: fixed-Ω_m assumption. Right: lensing-proxy-Ω_m assumption.

4 Interpretation

Under the physical-signal hypothesis, the model predicts upward pressure on GR-inferred early/high-z H_0 and non-negligible local-versus-high-z tension relief, but not a standalone full resolution. The late-time constrained endpoint remains moderate, and CMB-facing tests indicate detectable but model-dependent signatures that require full perturbation-level treatment for definitive statements.

Reproducibility

Core scripts used in this follow-up:

- `scripts/run_hubble_tension_mg_forecast.py`
- `scripts/run_hubble_tension_mg_forecast_robustness_grid.py`
- `scripts/run_hubble_tension_bias_transfer_sweep.py`
- `scripts/run_hubble_tension_final_relief_posterior.py`
- `scripts/run_joint_transfer_bias_fit.py`
- `scripts/run_hubble_tension_cmb_forecast.py`
- `scripts/run_hubble_tension_early_universe_bias.py`

Data Availability and DOIs

The follow-up uses posterior products from the O3 anomaly pipeline and public cosmology datasets. Data provenance and DOIs are:

- O3 modified-gravity tension replication repository (Zenodo): DOI 10.5281/zenodo.18584705.
- O3 search-sensitivity injection data used in upstream calibration (Zenodo): DOI 10.5281/zenodo.7890437.
- GWTC-3 catalog paper: DOI 10.1103/PhysRevX.13.041039.

- Pantheon+ cosmology constraints: DOI 10.3847/1538-4357/ac8e04.
- SH0ES local-H_0 reference: DOI 10.3847/2041-8213/ac5c5b.
- SDSS DR12 BOSS consensus BAO (source of `sdss_DR12Consensus_bao.dat`): DOI 10.1093/mnras/stx721.
- eBOSS DR16 cosmological compilation (source class for `sdss_DR16_LRG_BAO_DMDH.dat`): DOI 10.1103/PhysRevD.103.083533.
- DESI 2024 BAO cosmological constraints (source class for `desi_2024_gaussian_bao_ALL_GCcomb_mean.txt`): DOI 10.1088/1475-7516/2025/02/021.
- Cosmic-chronometer compilation components used in `Hz_BC03_all.dat`: DOIs 10.1088/1475-7516/2012/08/006, 10.1103/PhysRevD.71.123001, and 10.1088/1475-7516/2010/02/008.
- Planck 2018 cosmological parameters and lensing references: DOIs 10.1051/0004-6361/201833910 and 10.1051/0004-6361/201833886.

References

[1] A. B. Smith, "O3 Modified Gravity Tension Replication," Zenodo (2026), DOI: 10.5281/zenodo.18584705.

[2] LIGO Scientific Collaboration, Virgo Collaboration, and KAGRA Collaboration, "GWTC-3: Compact Binary Coalescences Observed by LIGO and Virgo During the Second Part of the Third Observing Run — O3 search sensitivity estimates," Zenodo (2023), DOI: 10.5281/zenodo.7890437.

[3] R. Abbott *et al.* (LIGO Scientific Collaboration, Virgo Collaboration, and KAGRA Collaboration), "GWTC-3: Compact Binary Coalescences Observed by LIGO and Virgo During the Second Part of the Third Observing Run," *Phys. Rev. X* **13**, 041039 (2023), DOI: 10.1103/PhysRevX.13.041039.

[4] D. Brout *et al.*, "The Pantheon+ Analysis: Cosmological Constraints," *Astrophys. J.* **938**, 110 (2022), DOI: 10.3847/1538-4357/ac8e04.

[5] A. G. Riess *et al.*, "A Comprehensive Measurement of the Local Value of the Hubble Constant with 1 km s^{-1} Mpc^{-1} Uncertainty from the Hubble Space Telescope and the SH0ES Team," *Astrophys. J. Lett.* **934**, L7 (2022), DOI: 10.3847/2041-8213/ac5c5b.

[6] S. Alam *et al.*, "The clustering of galaxies in the completed SDSS-III Baryon Oscillation Spectroscopic Survey: cosmological analysis of the DR12 galaxy sample," *Mon. Not. R. Astron. Soc.* **470**, 2617 (2017), DOI: 10.1093/mnras/stx721.

[7] S. Alam *et al.*, "Completed SDSS-IV extended Baryon Oscillation Spectroscopic Survey: Cosmological implications from two decades of spectroscopic surveys at the Apache Point Observatory," *Phys. Rev. D* **103**, 083533 (2021), DOI: 10.1103/PhysRevD.103.083533.

[8] DESI Collaboration, "DESI 2024 VI: cosmological constraints from the measurements of baryon acoustic oscillations," *J. Cosmol. Astropart. Phys.* **02** (2025) 021, DOI: 10.1088/1475-7516/2025/02/021.

[9] M. Moresco *et al.*, “Improved constraints on the expansion rate of the Universe up to $z \sim 1.1$ from the spectroscopic evolution of cosmic chronometers,” *J. Cosmol. Astropart. Phys.* **08** (2012) 006, DOI: 10.1088/1475-7516/2012/08/006.

[10] J. Simon, L. Verde, and R. Jimenez, “Constraints on the redshift dependence of the dark energy potential,” *Phys. Rev. D* **71**, 123001 (2005), DOI: 10.1103/PhysRevD.71.123001.

[11] D. Stern *et al.*, “Cosmic chronometers: constraining the equation of state of dark energy. I: $H(z)$ measurements,” *J. Cosmol. Astropart. Phys.* **02** (2010) 008, DOI: 10.1088/1475-7516/2010/02/008.

[12] N. Aghanim *et al.* (Planck Collaboration), “Planck 2018 results. VI. Cosmological parameters,” *Astron. Astrophys.* **641**, A6 (2020), DOI: 10.1051/0004-6361/201833910.

[13] N. Aghanim *et al.* (Planck Collaboration), “Planck 2018 results. VIII. Gravitational lensing,” *Astron. Astrophys.* **641**, A8 (2020), DOI: 10.1051/0004-6361/201833886.

[14] E. Belgacem, Y. Dirian, S. Foffa, and M. Maggiore, “Modified gravitational-wave propagation and standard sirens,” *Phys. Rev. D* **98**, 023510 (2018), DOI: 10.1103/PhysRevD.98.023510.

[15] A. Nishizawa, “Generalized framework for testing gravity with gravitational-wave propagation,” *Phys. Rev. D* **97**, 104037 (2018), DOI: 10.1103/PhysRevD.97.104037.